Nuclear Data for Science and Technology (1988 MITO), 67- 70, Copyright © 1988 JAERI.

MEASUREMENTS OF keV-NEUTRON CAPTURE GAMMA-RAY SPECTRA OF Fe AND Ni

Masayuki Igashira, Hiroshi Matsumoto, Toshio Uchiyama and Hideo Kitazawa

Research Laboratory for Nuclear Reactors, Tokyo Institute of Technology
2-12-1 O-okayama, Meguro-ku, Tokyo 152, Japan

Abstract: We have measured capture gamma-ray spectra of Fe and Ni at several neutron energies between 10 and 600 keV with an anti-Compton NaI(Tl) detector, employing a time-of-flight technique. Observed pulse-height spectra were unfolded using a response matrix of the detector in order to obtain capture gamma-ray spectra. Strong transitions from capture states to low-lying excited states of the residual nuclei were observed in both gamma-ray spectra. These spectra were compared with statistical model calculations. The calculation underestimates the strong transitions, but as a whole it reproduces fairly well the observed spectra at neutron energies of several hundreds keV.

(capture gamma-ray spectrum, keV neutron, Fe, Ni, statistical model calculation)

Introduction

Neutron-induced photon-production nuclear data are indispensable for shielding design calculation, for radiation damage estimate, and for radiation heating calculation. However, the data are scanty, especially in the keV-neutron region. On technological applications, the photon-production data contained in nuclear data libraries, e.g. ENDF/B, are not always satisfactory both in quantity and in quality. More accurate data are strongly requested for a new photon-production data library. Therefore, we have measured keV-neutron capture gamma-ray spectra of structural materials to provide these nuclear data and also to investigate the characteristics of resonance average spectra. The present paper reports on the results of Fe and Ni.

Experimental Procedure and Data Processing

Employing a time-of-flight(TOF) technique, neutron capture experiments were carried out. The experimental and data-processing methods have been described in detail elsewhere/1-3/ and are summarized briefly in the present paper. A pulsed proton beam (width: 1.5 ns FWHM, repetition rate: 2 MHz, average beam current: 10 μA) from the 3.2-MV Pelletron accelerator of the Research Laboratory for Nuclear Reactors in Tokyo Institute of Technology produced keV neutrons via the $^{7}Li(p,n)^{7}Be$ reaction. Capture samples were natural metallic disks of 60 mm in diameter and 5 mm in thickness, and were located at a distance of 150 mm from the neutron source. Capture gamma rays from the sample were detected by a 76 mmϕ×152mm NaI(Tl) detector centered in an annular NaI(Tl) detector, whose size is 254 mm in outer diameter and 280 mm in length. The detector assembly operated as an anti-Compton gamma-ray spectrometer and was placed in a heavy shield consisting of borated paraffin, lead and cadmium. A ^{6}LiH shield, which absorbed effectively neutrons scattered by the capture sample, was inserted into the collimeter of the detector shield. The distance between the sample and spectrometer was about 80 cm. Gamma rays were observed at an angle of 125° with respect to the proton beam direction, because the second Legendre polynomial is zero at this angle, and so the differential measurement at this angle produces approximately the total gamma-ray spectrum. Two ^{6}Li-glass scintillation detectors were used as neutron monitors. One detector, located at an angle of 7° with respect to the proton beam direction, was used to measure the incident neutron spectrum on a capture sample. The other detector located at -45° was used to monitor the number of neutrons emitted from the source. Capture gamma-ray measurements were performed at several neutron energies between 10 and 600 keV for both samples, and each running time was 35-60 h. The neutron energy spread was 6-70 keV.

A typical TOF spectrum for the Ni sample is shown in fig.1. The peak 'b' shows the capture gamma rays produced by the direct neutrons from the neutron source to the sample, and the peak 'a' shows the gamma rays produced by the $^{7}Li(p,\gamma)^{8}Be$ and $^{7}Li(p,p'\gamma)^{7}Li$ reactions. The part 'A' can be regarded as the nearly time-independent background, which mainly consists of the natural background and the gamma rays due to the $^{1}H(n_{th},\gamma)^{2}H$ and $^{56}Fe(n_{th},\gamma)^{57}Fe$ reactions in the detector shield. The time resolution of the gamma-ray detector system was about 4 ns(FWHM) and a good signal-to-noise ratio was obtained.

Signals from the gamma-ray detector were taken in a mini-computer as two-dimensional data (pulse-height and TOF), and the gamma-ray pulse-height spectrum corresponding to each of four digital windows set on the TOF spectrum was stored. One of the windows was set at the part

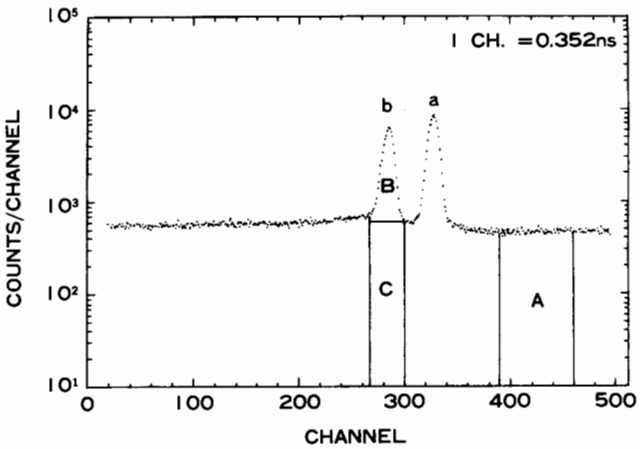

Fig. 1 Time-of-flight spectrum for the Ni sample at the neutron energy of 550 keV.

'B+C' in fig.1 to measure the capture gamma rays from the sample, and the other three windows were set in the part 'A' to determined the background(C). The net capture gamma-ray pulse-height spectrum was obtained by subtracting the background(C) from the foreground(B+C). As an example, a net pulse-height spectrum for the Ni sample is shown in fig. 2. Complicated structure is observed in high- and low-energy regions.

The capture gamma-ray pulse-height spectrum was unfolded by the computer code FERDOR/4/, using a response matrix of the detector which was constructed by an interpolation method from experimentally determined response functions/3/. Each response function has a simple shape with a strong full-energy peak and a weak single-escape peak, because our anti-Compton spectrometer rejects 80 % of Compton-scattering events, 95 % of single-escape events, and almost completely double-escape events. Diagonal elements of the response matrix are one to two orders greater than off-diagonal elements, so that the error occurring in spectrum unfolding is expected to be very small. The unfolded capture gamma-ray spectrum $\nu(E_\gamma)$ (gamma rays/capture/MeV) was normalized as

$$\int E_\gamma \cdot \nu(E_\gamma) dE_\gamma = \overline{Bn} + En$$

$$\overline{Bn} \equiv \sum_i A_i \frac{\langle \Gamma_{\gamma 0} \rangle_i}{\langle D_0 \rangle_i} Bn_i \Big/ \sum_i A_i \frac{\langle \Gamma_{\gamma 0} \rangle_i}{\langle D_0 \rangle_i}$$

where A_i is the natural abundance of the ith isotope, Bn_i the neutron binding energy, $\langle D_0 \rangle_i$ the s-wave average level spacing, $\langle \Gamma_{\gamma 0} \rangle_i$ the average radiative width for s-wave resonances, En the incident neutron energy, and E_γ the gamma-ray energy/5/. Correction for the gamma-ray attenuation in the sample was made by a Monte-Carlo calculation.

Results and Discussion

Measured capture gamma-ray spectra of Fe and Ni are shown in figs. 3 and 4, respectively. The spectrum hardness is characteristic of both spectra. Structure observed in the unfolded spectra can be attributed to the intrinsic one of the spectra, never to the oscillation generated from the unfolding process used in the present analysis. (Compare the spectrum of Ni at the neutron energy of 550 keV with the corresponding pulse-height spectrum shown in fig. 2.) The errors shown in the figures contain the statistical error, the error of the gamma-ray detector efficiency, and the error in the spectrum unfolding. The error in the spectrum normalization is not included. However, it was estimated to be less than about 5 %.

In fig. 3, the strong transitions($E_\gamma \approx 8$ MeV) from capture states to the ground state and/or first excited state of ^{57}Fe are observed. The sum intensity of these transitions ranges between 0.25 and 0.34 (gamma rays/capture). The spectrum in the neutron-energy region of 24-31 keV virtually consists of the gamma rays from the 27.7-keV s-wave neutron resonance capture by ^{56}Fe. The total radiative width of this resonance has been measured to be 1.06 eV by Wisshak et al./6/. This value produces the partial radiative width of 0.36 eV for the above observed intensity(0.34). This width is in good agreement with the corresponding value, 0.31 eV, of Komano et al./7/, who have measured the partial radiative widths for the ground state and first excited state with a Ge detector. The gamma rays higher than 8.5 MeV result from the capture by the minor isotopes(^{54}Fe and ^{57}Fe).

The spectra of Ni shown in fig. 4 also exhibit strong transitions from capture states to low-lying states of the residual nuclei. The intensity of the gamma rays higher than 7 MeV ranges between 0.56 and 0.72 (gamma rays/capture).

Barrett et al. have measured keV-neutron capture gamma-ray spectra of Fe and Ni/8/, however their gamma-ray energy resolution was too low to make a comparison with our data.

The capture gamma-ray spectra of Fe and Ni were calculated by the computer code CASTHY/9/

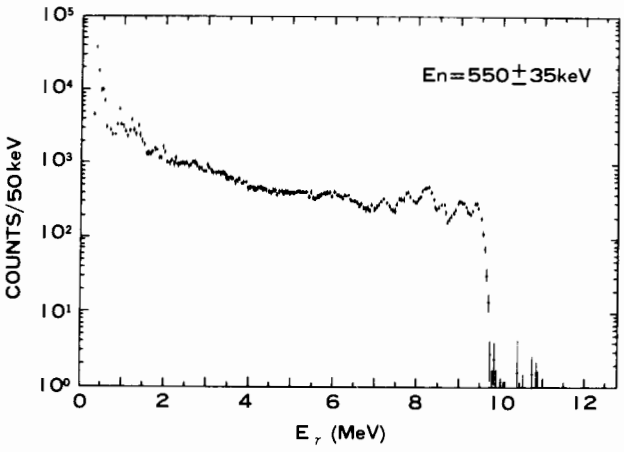

Fig. 2 Background-subtracted capture gamma-ray pulse-height spectrum of Ni at the neutron energy of 550 keV.

Table 1. Nuclear level-density parameters used for the statistical model calculation

Nuclei	a (MeV^{-1})	Ex (MeV)	T (MeV)	$\sigma^2(0)$	Δ (MeV)
^{55}Fe	7.35	8.5	1.23	12.3	1.54
^{57}Fe	8.68	7.5	1.13	3.46	1.54
^{59}Ni	7.34	8.5	1.26	6.25	1.2
^{61}Ni	8.27	7.5	1.15	4.0	1.2
^{62}Ni	8.08	8.2	1.07	6.25	2.61

The quantities a are the level-density parameter in the Fermi-gas-model formula, T are the nuclear temperature in the constant-temperature-model formula, Ex are the energy connecting both formulas, $\sigma^2(0)$ are the spin-cutoff factor in the vicinity of the ground state, and Δ are the pairing energy.

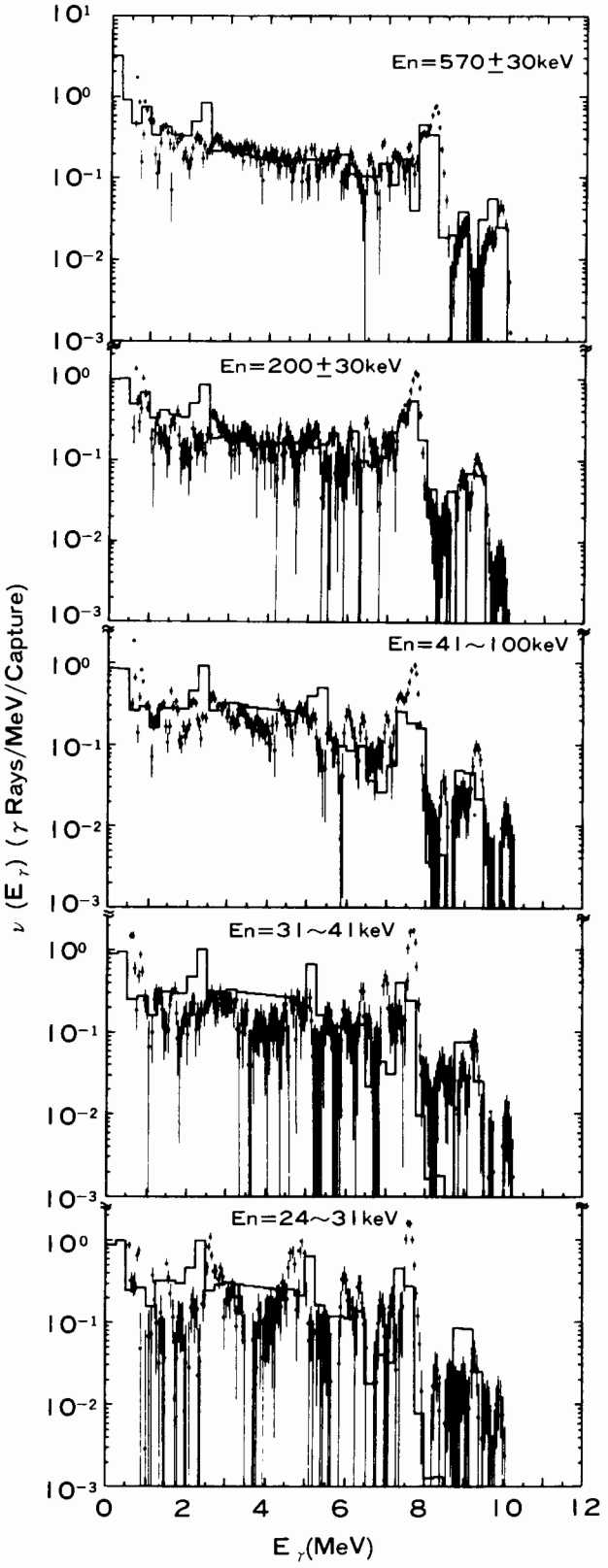

Fig. 3 Unfolded capture gamma-ray spectra of Fe. Incident-neutron energies are shown in the figures. The histograms show the spectra calculated by the statistical model. The calculation was made at the mean energy in each incident-neutron energy region.

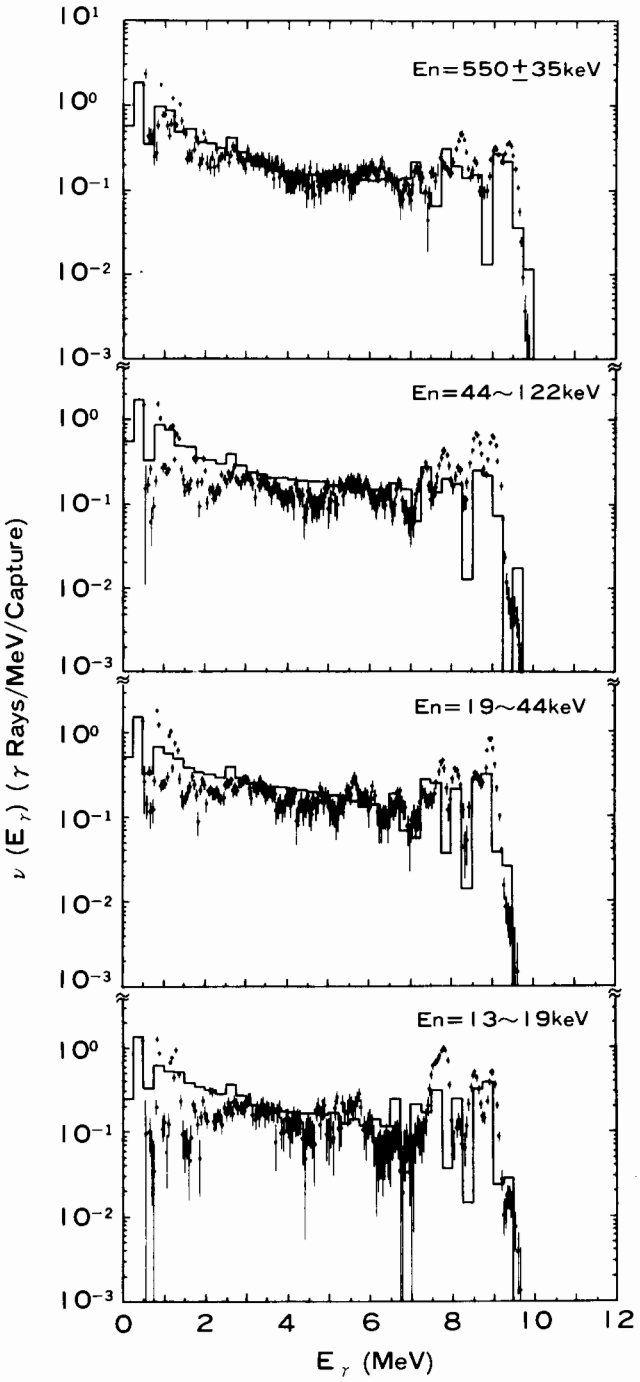

Fig. 4 Unfolded capture gamma-ray spectra of Ni. Incident-neutron energies are shown in the figures. The histograms show the spectra calculated by the statistical model. The calculation was made at the mean energy in each incident-neutron energy region.

based on the Hauser-Feshbach statistical model. The calculation includes electric-dipole(E1), magnetic-dipole(M1), and electric-quadrupole(E2) transition. The conventional Brink-Axel gamma-ray strength function was used for the E1 transition, and the parameters of the giant E1 resonance were taken from the compilation of Berman/10/. For the M1 and E2 transitions, the single-particle transitions of Weisskopf were assumed. The composite formula proposed by Gilbert-Cameron/11/ was used for a nuclear level-density distribution in the calculation. The nuclear level-density parameters were determined from a cumulative plot of the number of excited levels and from the s-wave average level spacing at the neutron binding energy/5/. The determined parameters for the residual nuclei are shown in table 1. In the intermediate energy region between the vicinity of the ground state and Ex, the spin-cutoff factors were obtained by a linear interpolation between $\sigma^2(0)$ and $\sigma^2(Ex)$, where $\sigma^2(Ex)=0.146(a\cdot Ex)^{1/2}A^{2/3}$. Major target isotopes and some of minor target isotopes, ^{54}Fe, ^{56}Fe, ^{58}Ni, ^{60}Ni, and ^{61}Ni, were included in the calculations. Here, the capture gamma-ray spectrum of natural iron or nickel was obtained by summing up the weighted spectrum of each isotope, which was calculated using the weight factor consisting of the natural abundance, the average radiative width for s-wave resonances, and the s-wave average level spacing/5/.

In the calculation of Fe, for lack of the data, the giant E1 resonance parameters of ^{55}Mn were substituted for the ones of ^{55}Fe and ^{57}Fe. Similarly, the resonance parameters of ^{60}Ni were substituted for the ones of ^{59}Ni, ^{61}Ni, and ^{62}Ni. To check on the effect of the ambiguity of giant E1 resonance parameters, the calculation of Fe using the resonance parameters of ^{60}Ni was performed. However, the change of the spectrum was negligibly small. It means that only the functional form of the E1 strength function is essential in the present calculation, provided that reasonable parameters of the giant E1 resonance are used. On the other hand, the uncertainty of nuclear level-density parameters is strongly propagated to the calculated spectra. The s-wave average level spacings used in determining the level-density parameters contain errors ranging between 12 and 17 %, and the statistical uncertainty of the cumulative plot of the number of excited levels seems to be about 10 %. Therefore, the uncertainty of the calculated spectra resulting from the ambiguity of the level-density parameters is estimated to be 15-20 %.

The calculated spectra of Fe are shown by the histograms in fig. 3. The calculation reproduces fairly well the observed spectra at the neutron energies of 200 and 570 keV as a whole, but it does not reproduce the complicated spectra at the lower incident-neutron energies. (The spectrum at the neutron energy region of 24-31 keV virtually consists of the gamma rays from the 27.7-keV s-wave neutron resonance capture by ^{56}Fe, as described above. Therefore, the comparison between the observed and calculated spectra might be somewhat meaningless.) Moreover, the calculation underestimates the gamma rays around 8 MeV mentioned above, but the discrepancy becomes small in the spectra at the higher incident-neutron energies. The gamma rays around 10 MeV in the observed spectra at lower incident-neutron energies are scarcely reproduced, because these gamma rays result from the capture by ^{57}Fe which was neglected in the calculation. The peak around 2.3 MeV in the calculated spectra results from the transitions between the discrete levels taken into account in the calculation, but the corresponding strong peak does not appear in the observed spectra.

The calculated spectra of Ni are shown by histograms in fig. 4. The calculation reproduces fairly well the observed spectrum at the neutron energy of 550 keV as a whole, but the reproduction is not good at the lower incident-neutron energies. Moreover, the high-energy gamma rays(E_γ>7.5 MeV) are underestimated in all spectra, although the discrepancy in the spectrum at the neutron energy of 550 keV is small. These situations are very similar to those in the Fe results.

Summary

We have measured capture gamma-ray spectra of Fe and Ni at neutron energies of 10 to 600 keV. The strong transitions from capture states to the ground state and/or first excited state of ^{57}Fe were observed in the spectra of Fe, and the sum intensity of these transitions at the neutron energy region of 24-31 keV is quite consistent with the partial radiative widths of Komano et al. In the spectra of Ni, strong transitions from capture states to low-lying excited states of the residual nuclei were also observed. The statistical-model calculation did not explain these strong transitions in both spectra, but as a whole it reproduced fairly well the spectra at neutron energies of several hundreds keV.

The authors acknowledge H. Anze, Y. Dozono, and Y. Lee of our laboratory for their help to the experiments and data analysis.

REFERENCES

1. M. Igashira, H. Kitazawa and N. Yamamuro: Nucl. Instr. and Meth. A245, 432(1986)
2. M. Shimizu, M. Igashira, K. Terazu and H. Kitazawa: Nucl. Phys. A452, 205(1986)
3. M. Igashira, H. Kitazawa, M. Shimizu, H. Komano and N. Yamamuro: Nucl. Phys. A457, 301(1986)
4. H. Kendrick and S.M. Sperling: GA-9882(1970)
5. S.F. Mughabghab, M. Divadeenum and N. E. Holden: Neutron Cross Sections, vol. 1, part A (Academic Press, New York, 1981)
6. K. Wisshak, F. Käppeler, G. Reffo and F. Fabbri: Nucl. Sci. Eng. 86, 168(1984)
7. H. Komano, M. Igashira, M. Shimizu and H. Kitazawa: Phys. Rev. C29, 345(1984)
8. R.F. Barrett, K.H. Bray, B.J. Allen and M.J. Kenny et al.: Nucl. Phys. A278, 204(1977)
9. S. Igarasi: J. Nucl. Sci. Technol. 12, 67(1975)
10. B.L. Berman: Atom. Data and Nucl. Data Table, 15, 319(1975)
11. A. Gilbert and A.G.W. Cameron: Can. J. Phys. 43, 1446(1965)